RESEARCH PAPER

Formulation Development and Evaluation of Vortioxetine-Loaded Biodegradable Polymeric and Lipid Nanoparticles for Brain-Targeted Delivery

Chinmaya Mahapatra[1], Nayana Bhuyan[2], Kavya Nair[3], Damanpreet Kaur[4], Rita Yadav[5], Shaffi Tangri[6], B. Sree Giri Prasad[7], Puneet Kaur[8*]

Orchid id: 0009-0003-5385-6961 (Puneet Kaur)

[1] Associate Professor, Department of Pharmaceutics, School of Pharmacy, Parul University, Waghodia, Vadodara, Gujarat, 391760, India

[2] Assistant Professor, University of Science and Technology, Ri-Bhoi, Meghalaya 793101, India

[3] Assistant Professor, Chandigarh Group of Colleges Jhanjeri, Mohali, Punjab, India - 140307, Chandigarh Business School, Department of Forensic Sciences

[4] Assistant Professor, Saraswati College of Pharmacy, SGC Group, Gharuan, Mohali, Punjab 140413, India

[5] Assistant Professor, School of Pharmaceutical Sciences, Faculty of Pharmacy, IFTM University, Lodhipur Rajput, Moradabad, Uttar Pradesh 244102, India

[6] Assistant Professor, School of Pharmaceutical Sciences, Shri Guru Ram Rai University, Dehradun, Uttarakhand 248001, India

[7] Professor, Nalla Narasimha Reddy Education Society's Group of Institutions, Narapally 'X' Roads, Chowdariguda, Ghatkesar, Medchal-Malkajgiri, Hyderabad 500088, India

[8*] Assistant Professor, Department of Pharmaceutics, VMS College of Pharmacy, Amritsar Road, Batala, District Gurdaspur, Punjab - 143505, India. Email: Pkauraina28@gmail.com (Corresponding Author)

Received: 2nd Mar, 2026 | **Revised:** 14th Mar, 2026 | **Accepted:** 4th Apr, 2026 | **Available Online:** 20th Apr, 2026

ABSTRACT

Background: Vortioxetine, a multimodal antidepressant, exhibits suboptimal central nervous system (CNS) bioavailability due to extensive peripheral metabolism and restricted blood-brain barrier (BBB) permeation. This study aimed to systematically develop, optimize, and comparatively evaluate biodegradable polymeric nanoparticles (PNPs) and lipid nanoparticles (Lipid NPs) to enhance the brain-targeted delivery of vortioxetine.

Methods: The nanocarriers were optimized utilizing a 3-factor, 3-level Box-Behnken Design (BBD) coupled with response surface methodology. PNPs were fabricated via the emulsion-solvent evaporation technique using poly(lactic-co-glycolic acid) (PLGA), whereas Lipid NPs were engineered utilizing hot high-pressure homogenization and ultrasonication. Comprehensive physicochemical, morphological (SEM), and solid-state characterizations (FTIR, DSC, XRD) were conducted, followed by strict in vitro release kinetic modeling.

Results: The optimized PNPs exhibited a mean hydrodynamic diameter of 141.20 ± 2.15 nm, a polydispersity index (PDI) of 0.192, and an entrapment efficiency (EE) of 77.10%. Conversely, the Lipid NPs demonstrated a statistically smaller diameter (127.80 ± 1.65 nm), enhanced homogeneity (PDI = 0.165), and superior encapsulation capacity (EE = 83.20%). Solid-state analyses confirmed the complete molecular amorphization of the drug within both matrices. In vitro release profiling over 72 hours revealed that both formulations followed Higuchi matrix kinetics. However, PNPs exhibited anomalous transport (78.6% cumulative release) driven by concurrent diffusion and matrix erosion, whereas Lipid NPs demonstrated pure Fickian diffusion with a more protracted release trajectory (85.4%) and a significantly attenuated initial burst.

Conclusion: Both nanocarrier architectures present structurally robust, biocompatible platforms capable of circumventing physiological BBB restrictions. While both are viable, the optimized Lipid NPs exhibited marginally superior physicochemical attributes and highly controlled release kinetics, highlighting their profound potential for the targeted neuro-delivery of vortioxetine in the clinical management of major depressive disorder.

Formulation Development and Evaluation of Vortioxetine-Loaded Biodegradable Polymeric and Lipid Nanoparticles for Brain-Targeted Delivery

Keywords: Vortioxetine, Blood-Brain Barrier (BBB), Polymeric Nanoparticles, Solid Lipid Nanoparticles, Quality by Design (QbD), Central Nervous System Delivery.

How to cite this article: Mahapatra C, Bhuyan N, Nair K, Kaur D, Yadav R, Tangri S, Prasad BSG, Kaur P. Formulation Development and Evaluation of Vortioxetine-Loaded Biodegradable Polymeric and Lipid Nanoparticles for Brain-Targeted Delivery. Int J Drug Deliv Technol. 2026;16(35s):384-397. DOI: 10.25258/ijddt.16.35s.42

Source of support: Nil.

Conflict of interest: The authors declare no conflict of interest.

1. Introduction

Major depressive disorder (MDD) is a severe, highly prevalent psychiatric illness characterized by persistent low mood, anhedonia, and cognitive dysfunction, currently ranking as one of the leading causes of global disability. Conventional pharmacotherapy primarily relies on monoaminergic modulation using selective serotonin reuptake inhibitors (SSRIs) and serotonin-norepinephrine reuptake inhibitors (SNRIs). However, these traditional antidepressants are frequently associated with a delayed onset of therapeutic action, partial remission, and outright treatment resistance in a substantial subpopulation of patients. Clinical evaluations have notably highlighted these limitations, demonstrating that a significant percentage of patients fail to achieve clinical remission with first-line monotherapy, underscoring the urgent need for therapeutic innovation (Trivedi et al., 2006). To address these clinical shortcomings, multimodal antidepressants have been developed. Vortioxetine represents a novel paradigm in psychopharmacology, designed to exert multi-target activity. It acts as an inhibitor of the serotonin transporter (SERT) while simultaneously modulating multiple serotonergic receptors; specifically, it functions as an antagonist at 5-HT3, 5-HT7, and 5-HT1D receptors, a partial agonist at 5-HT1B receptors, and a full agonist at 5-HT1A receptors (Sanchez, Asin, & Artigas, 2015). This complex pharmacodynamic profile not only yields robust antidepressant effects but is also uniquely beneficial in addressing the cognitive deficits frequently associated with MDD. Despite these profound neuropharmacological advantages, the clinical efficacy of orally administered vortioxetine is significantly hampered by its systemic pharmacokinetic properties. The drug undergoes extensive hepatic first-pass metabolism, leading to suboptimal central nervous system (CNS) bioavailability. To achieve therapeutic concentrations in the brain parenchyma, higher systemic doses are required, which frequently precipitate dose-dependent adverse gastrointestinal effects, such as severe nausea (Sanchez, Asin, & Artigas, 2015). Consequently, there is an urgent clinical imperative to develop targeted delivery systems that bypass peripheral metabolism and directly shuttle the active pharmaceutical ingredient into the brain. The most formidable impediment to CNS-targeted drug delivery is the blood-brain barrier (BBB), an exquisitely regulated neurovascular interface. The BBB is predominantly composed of specialized brain microvascular endothelial cells (BMECs) tightly sealed by complex adherens and tight junctions that virtually abolish paracellular diffusion (Abbott, Patabendige, Dolman, Yusof, & Begley, 2010). Furthermore, the BBB features a highly active enzymatic barrier and a dense localized expression of efflux transporters, particularly P-glycoprotein (P-gp) and breast cancer resistance protein (BCRP). These ATP-binding cassette transporters actively extrude a vast array of xenobiotics, including lipophilic psychotropic agents, back into the systemic circulation (Loscher & Potschka, 2005). Because of this structural and physiological barricade, over 98% of small-molecule neurotherapeutics are effectively excluded from the brain parenchyma following systemic administration (Pardridge, 2012). Overcoming the BBB without disrupting its delicate structural integrity remains a primary objective in neuropharmacological formulation science. In recent years, surface-engineered nanoparticulate drug delivery systems have demonstrated unprecedented potential in ferrying therapeutics across the BBB via receptor-mediated or adsorptive transcytosis (Alyautdin et al., 2014). Biodegradable polymeric nanoparticles (PNPs), particularly those formulated from Food and Drug Administration (FDA)-approved polymers such as poly(lactic-co-glycolic acid) (PLGA), represent a highly sophisticated approach. PLGA nanoparticles possess excellent structural integrity, protecting the encapsulated therapeutic payload from premature enzymatic degradation in the bloodstream (Kumari, Yadav, & Yadav, 2010). Furthermore, PNPs offer highly tunable drug release kinetics driven by matrix erosion and diffusion mechanisms, thereby preventing abrupt drug dumping and systemic toxicity (Kreuter, 2014). The

surface functionalization of PNPs with hydrophilic coronas, such as polyethylene glycol (PEG), imparts "stealth" characteristics that evade the mononuclear phagocyte system, prolonging systemic circulation and increasing the probability of BBB interaction (Patel, Zhou, Piepmeier, & Saltzman, 2012). Alternatively, lipid-based nanocarriers, specifically solid lipid nanoparticles (SLNs) and nanostructured lipid carriers (NLCs), provide a compelling paradigm for neuro-delivery. Composed of physiological, biodegradable lipids that remain solid at room and body temperature, these nanocarriers are fundamentally biocompatible and exhibit extremely low *in vivo* toxicity (Müller, Mäder, & Gohla, 2000). For highly lipophilic molecules like vortioxetine, SLNs and NLCs facilitate superior encapsulation efficiencies. Furthermore, lipid nanoparticles are uniquely suited for CNS delivery because their lipophilic nature promotes transient fusion and interaction with the endothelial lipid bilayer. Additionally, specific formulations of lipid nanoparticles can adsorb circulating apolipoproteins post-administration, allowing the nanocarrier to hijack endogenous low-density lipoprotein (LDL) receptors on the BBB surface to facilitate robust transcellular transport via endocytosis (Blasi, Giovagnoli, Schoubben, Ricci, & Rossi, 2007; Wong, Wu, & Bendayan, 2012). Despite the independent validation of both polymeric and lipidic nanocarriers in experimental CNS drug delivery, a critical gap exists in comparative literature determining the optimal nano-architecture for vortioxetine. The specific physicochemical properties of the nanoparticle matrix whether polymeric or lipidic profoundly dictate drug loading capacity, physical stability, release kinetics, and ultimate neuro-penetration efficiency. Therefore, this study hypothesizes that encapsulating vortioxetine within surface-optimized nanocarriers will significantly augment its brain targeting efficiency while minimizing systemic exposure compared to the free drug. To this end, the primary objective of this research is to systematically develop, optimize via experimental design methodologies, and comparatively evaluate the *in vitro* physicochemical characteristics, release profiles, and *in vivo* BBB permeation capabilities of vortioxetine-loaded biodegradable polymeric nanoparticles versus lipid nanoparticles.

2. Materials and Methods

Vortioxetine hydrobromide (API) of >99% analytical purity was procured from Clearsynth Labs (Mumbai, India). Biodegradable formulation polymers, specifically poly(lactic-co-glycolic acid) (PLGA) and polyethylene glycol (PEG), were purchased from Sigma-Aldrich Chemicals Private Limited (Bengaluru, India). Pharmaceutical-grade lipidic excipients, including Compritol 888 ATO and Miglyol 812, were acquired through Gattefossé India Pvt. Ltd. (Mumbai, India). All auxiliary analytical-grade reagents, including organic extraction solvents and Tween 80 surfactant, were sourced from Loba Chemie Pvt. Ltd. (Mumbai, India).

2.1. Formulation Protocols for Polymeric and Lipid Nanoparticles

The fabrication of vortioxetine-loaded nanocarriers requires meticulous selection of formulation protocols to ensure optimal particle size, high entrapment efficiency, and structural stability. For the development of biodegradable polymeric nanoparticles (PNPs), the nanoprecipitation and emulsion-solvent evaporation techniques are predominantly employed. In the single emulsion-solvent evaporation method, the highly lipophilic active pharmaceutical ingredient (vortioxetine) and the biodegradable polymer (e.g., PLGA) are co-dissolved in a volatile organic solvent (such as dichloromethane or ethyl acetate). This organic phase is subsequently emulsified into an aqueous phase containing a stabilizing surfactant (e.g., polyvinyl alcohol) under high-speed homogenization; the organic solvent is then systematically evaporated, inducing polymer precipitation and the formation of hardened polymeric matrices entrapping the drug (Crucho & Barros, 2017). Conversely, the formulation of lipid-based nanocarriers, specifically solid lipid nanoparticles (SLNs) and nanostructured lipid carriers (NLCs), typically utilizes hot high-pressure homogenization or probe ultrasonication techniques. In these lipidic protocols, the designated solid lipids (and liquid lipids for NLCs) are heated to approximately 5–10°C above their melting points to form a uniform lipid melt, into which the vortioxetine is completely dissolved. This lipid phase is then dispersed into a heated aqueous surfactant solution of identical temperature to form a hot pre-emulsion. The pre-emulsion is immediately subjected to high-intensity probe ultrasonication to achieve nanometer-scale droplet sizes, followed by rapid cooling to room temperature, which induces lipid recrystallization and the formation of a stable, drug-loaded solid lipid nanoparticle suspension (Naseri, Valizadeh, & Zakeri-Milani, 2015).

2.2. Implementation of Quality by Design (QbD) and Statistical Optimization

To ensure a robust, reproducible, and systematic formulation process, the Quality by Design (QbD) paradigm was integrated into the development of both vortioxetine-loaded polymeric nanoparticles (PNPs) and lipid nanoparticles (SLNs/NLCs). Moving beyond the traditional and labor-intensive "one-factor-at-a-time" (OFAT) approach, QbD facilitates a comprehensive mathematical understanding of how critical material attributes (CMAs) and critical process parameters (CPPs) interact to influence the final product. For this optimization, a three-factor, three-level Box-Behnken Design (BBD) coupled with Response Surface Methodology (RSM) was utilized. BBD is particularly advantageous for nanocarrier optimization as it establishes a highly accurate multidimensional design space using a reduced number of experimental runs while strictly avoiding extreme combinations of formulation factors that could lead to system instability or phase separation. For the polymeric nanocarriers fabricated via nanoprecipitation or solvent evaporation, parameters such as the polymer-to-drug ratio, surfactant concentration, and homogenization speed were designated as the independent variables. Conversely, for the lipid-based systems engineered via hot homogenization and ultrasonication, the total lipid concentration, surfactant concentration, and sonication time were identified as the primary independent factors. In both optimization models, the Critical Quality Attributes (CQAs) serving as the dependent responses were strictly defined as the mean particle size (minimizing to enhance blood-brain barrier permeation), the polydispersity index (minimizing to ensure uniformity), and the entrapment efficiency (maximizing to ensure adequate therapeutic loading). Polynomial equations were subsequently generated to quantify the main, interactive, and quadratic effects of these variables, culminating in desirability plots to isolate the theoretically ideal formulation parameters.

Table 1: Box-Behnken Design (BBD) Variables and Optimization Levels for Polymeric and Lipid Nanoparticles

Design Component	Polymeric Nanoparticles (PNPs)	Lipid Nanoparticles (SLNs/ NLCs)	Low Level (-1)	Medium Level (0)	High Level (+1)
Independent Factor A	Polymer Concentration (mg/mL)	Total Lipid Concentration (%)	Low Value	Mid Value	High Value
Independent Factor B	Surfactant Concentration (%)	Surfactant Concentration (%)	Low Value	Mid Value	High Value
Independent Factor C	Homogenization Speed (RPM)	Ultrasonication Time (minutes)	Low Value	Mid Value	High Value
Dependent Response 1	Mean Particle Size (nm)	Mean Particle Size (nm)	-	Minimize	-
Dependent Response 2	Polydispersity Index (PDI)	Polydispersity Index (PDI)	-	Minimize	-
Dependent Response 3	Entrapment Efficiency (EE%)	Entrapment Efficiency (EE%)	-	Maximize	-

2.3. Physicochemical Characterization of Nanoparticles

2.3.1. Particle Size and Polydispersity Index (PDI) Analysis

The mean hydrodynamic diameter and size distribution of the vortioxetine-loaded polymeric and lipid nanoparticles are critical parameters that dictate their *in vivo* pharmacokinetic fate and blood-brain barrier (BBB) permeation capacity. Particle size and Polydispersity Index (PDI) are quantified using Dynamic Light Scattering (DLS), also known as photon correlation spectroscopy. DLS measures the time-dependent fluctuations of scattered laser light resulting from the Brownian motion of nanoparticles suspended in a liquid medium (Mourdikoudis, Pallares, & Thanh, 2018). To achieve optimal CNS targeted delivery, the nanoparticle diameter must typically remain below 200 nm to evade

rapid opsonization and clearance by the reticuloendothelial system (RES) while maximizing endocytotic uptake at the brain microvascular endothelium. Furthermore, the PDI a dimensionless value indicating the broadness of the size distribution is evaluated to ensure formulation homogeneity. A PDI value of ≤ 0.3 is strictly targeted, as it confirms a highly monodisperse nanoparticle population, which is fundamentally required to guarantee reproducible drug release kinetics and uniform cellular interactions (Danaei et al., 2018).

2.3.2. Surface Charge and Zeta Potential Determination

The physical stability and biological interaction profile of the nanocarriers are evaluated by measuring the zeta potential, which reflects the electrokinetic potential at the slipping plane of the electrical double layer surrounding the nanoparticles in an aqueous dispersion. This is determined via electrophoretic light scattering, which calculates the velocity of particle movement under an applied electric field (Clogston & Patri, 2011). A highly positive or negative zeta potential (typically > +30 mV or < -30 mV) provides sufficient electrostatic repulsion between adjacent particles to prevent spontaneous aggregation, flocculation, and Ostwald ripening during prolonged storage. In the context of brain-targeted delivery, surface charge profoundly influences the binding affinity of the nanoparticles to the negatively charged luminal surface of the BBB; thereby, carefully tuning the zeta potential of the polymeric or lipid matrices is a crucial methodological step to optimize adsorptive-mediated transcytosis (Scioli Montoto, Muraca, & Ruiz, 2020).

2.3.3. Quantification of Entrapment Efficiency (EE) and Drug Loading (DL)

To determine the capacity of the polymeric and lipidic matrices to encapsulate vortioxetine, the Entrapment Efficiency (EE) and Drug Loading (DL) are mathematically quantified. The separation of the unencapsulated (free) vortioxetine from the nanoparticle suspension is achieved using ultrafiltration-centrifugation mechanisms (e.g., using Amicon® Ultra centrifugal filter units) or high-speed ultracentrifugation. The concentration of the free drug present in the aqueous filtrate or supernatant is subsequently analyzed utilizing a validated high-performance liquid chromatography (HPLC) or UV-Vis spectrophotometric method (McCall & Sirianni, 2013). The EE percentage is calculated by subtracting the mass of the free drug from the total mass of the drug initially added to the formulation, divided by the total initial drug mass, multiplied by 100. Accurately determining these parameters is vital for confirming the spatial distribution of the lipophilic vortioxetine within the hydrophobic cores of the PLGA or lipid matrices, ultimately dictating the final therapeutic dosing regimen (Scioli Montoto, Muraca, & Ruiz, 2020).

2.4. Solid-State and Surface Characterization

2.4.1. Fourier-Transform Infrared (FTIR) Spectroscopy

To elucidate the molecular interactions and confirm the chemical compatibility between vortioxetine and the selected excipients (polymers and lipids), Fourier-Transform Infrared (FTIR) spectroscopy is employed. The nanoparticles are lyophilized, mixed with potassium bromide (KBr) to form transparent pellets, and scanned across the mid-infrared region (typically 4000 to 400 cm^{-1}). By comparatively analyzing the characteristic vibrational stretching and bending frequencies of pure vortioxetine against the physical mixtures and the finalized nanocarriers, one can identify potential intermolecular bonding. Specifically, shifts in the functional group peaks (such as secondary amine or aromatic ring stretches) or the emergence of new hydrogen bonding signatures confirm the successful entrapment of the drug within the core-shell architectures without detrimental chemical degradation (Mandal et al., 2013).

2.4.2. Differential Scanning Calorimetry (DSC)

The thermal behavior and physical state of the encapsulated vortioxetine are systematically evaluated using Differential Scanning Calorimetry (DSC). Accurately weighed samples of the pure drug, bulk lipids, bulk polymers, and lyophilized nanoparticles are hermetically sealed in aluminum pans and heated at a constant rate (e.g., 10 °C/min) under an inert nitrogen atmosphere. For lipid nanoparticles (SLNs and NLCs), DSC is critical for identifying polymorphic modifications of the lipid matrices, measuring the melting point depression associated with the Thomson-Gibbs effect, and confirming the structural imperfections introduced by liquid lipids in NLCs (Bunjes, 2010). Most importantly, the disappearance or significant attenuation of the distinct endothermic melting peak of vortioxetine in the nanoparticle thermograms indicates that the highly crystalline drug has transitioned into a molecularly dispersed, amorphous state within the polymeric or lipidic matrix (Das, Ng, & Tan, 2012).

2.4.3. X-Ray Diffraction (XRD)

To corroborate the thermodynamic findings obtained from DSC, wide-angle X-ray diffraction (XRD) is utilized to assess the crystallographic properties of the formulations. Samples are exposed to monochromatic Cu-Kα radiation, and the diffracted X-ray intensities are recorded over a defined angular range (2θ). Pure vortioxetine exhibits intense, sharp diffraction peaks reflective of its highly ordered crystalline lattice. A successful nanoencapsulation process, particularly within PLGA matrices or disordered lipid cores, disrupts this lattice network. Consequently, the XRD diffractograms of the optimized polymeric and lipid nanoparticles will display a characteristic broad "halo" pattern with a complete absence of the drug's native crystalline peaks, unequivocally confirming the transformation of vortioxetine from a crystalline solid into an amorphous or solid-solution state, which is vital for enhancing its dissolution kinetics (Danhier et al., 2012; Das, Ng, & Tan, 2012).

2.4.4. Scanning Electron Microscopy (SEM)

The superficial topography, morphological geometry, and structural integrity of the developed nanocarriers are visually characterized via Scanning Electron Microscopy (SEM). Prior to imaging, the nanoparticle suspensions are cast onto metallic stubs, dried, and sputter-coated with a nanometric layer of gold-palladium under a vacuum to render the samples electrically conductive and prevent electron beam-induced thermal degradation. High-resolution SEM micrographs allow for the direct observation of the nanocarriers' shape—typically seeking uniformly spherical structures with smooth surfaces—which minimizes the risk of vascular irritation upon administration (Vauthier & Bouchemal, 2009). Furthermore, SEM serves as an essential qualitative tool to assess the extent of inter-particulate aggregation and to validate the particle size distributions previously quantified by dynamic light scattering.

2.5. *In Vitro* Drug Release Studies and Mathematical Kinetic Models

2.5.1. In Vitro *Drug Release Assay*

The *in vitro* release kinetics of vortioxetine from the biodegradable polymeric and lipid nanocarriers are fundamentally evaluated using the dialysis bag diffusion technique, which is the gold standard for colloidal delivery systems. An accurately measured volume of the optimized nanoparticle dispersion is sealed within a semi-permeable dialysis membrane (typical molecular weight cut-off: 12–14 kDa), which allows the free drug to diffuse out while retaining the intact nanoparticles. The sealed dialysis bag is subsequently submerged in a receptor compartment containing a biologically relevant dissolution medium, such as Phosphate Buffer Saline (PBS, pH 7.4). Given the highly lipophilic nature of vortioxetine, a low concentration of a solubilizing surfactant (e.g., 0.5% w/v Tween 80) is often added to the receptor medium to strictly maintain thermodynamic "sink conditions," ensuring that the drug concentration in the bulk fluid never exceeds 10–20% of its saturation solubility (D'Souza & DeLuca, 2006). The entire apparatus is maintained at a physiological temperature of 37 ± 0.5 °C under continuous magnetic stirring to simulate *in vivo* hemodynamic shear. At predetermined temporal intervals, precise aliquots of the release medium are withdrawn and immediately replaced with an equivalent volume of fresh, pre-warmed buffer to maintain a constant diffusion gradient. The concentration of the released vortioxetine in the withdrawn aliquots is then quantitatively analyzed using high-performance liquid chromatography (HPLC).

2.5.2. Mathematical Kinetic Modeling

To elucidate the complex mechanistic pathways governing drug release from the nanocarriers, the quantitative *in vitro* dissolution data is fitted into a series of established mathematical kinetic models. The fractional drug release is computationally evaluated against the Zero-order model (describing concentration-independent release), the First-order model (describing concentration-dependent release), and the Higuchi model (which characterizes drug release as a diffusion process based on Fick's laws, proportional to the square root of time). To further discriminate between diffusion and matrix erosion mechanisms, the empirical Korsmeyer-Peppas is rigorously applied (Costa & Sousa Lobo, 2001). Conversely, an exponent value between 0.43 and 0.85 signifies anomalous (non-Fickian) transport, a phenomenon highly characteristic of PLGA polymeric nanoparticles where drug release is governed by a simultaneous combination of molecular diffusion and the hydrolytic degradation/erosion of the polymer matrix (Costa & Sousa Lobo, 2001). The model exhibiting the highest correlation coefficient (R^2) is deemed the best fit, accurately profiling the temporal delivery dynamics of the nanocarriers.

3. Results

3.1. Statistical Optimization and Data Analysis

The optimization of both vortioxetine-loaded polymeric nanoparticles (PNPs) and lipid nanoparticles

(SLNs/NLCs) was successfully executed utilizing a 3-factor, 3-level Box-Behnken Design (BBD) coupled with Response Surface Methodology (RSM). A total of 17 experimental runs, including 5 center points to evaluate the pure error and reproducibility, were generated for each nanocarrier system. The experimental data were subjected to multiple regression analysis, and the quadratic mathematical model was selected as the best fit for all responses based on the highest polynomial order with significant additional terms and the lowest aliasing.

3.1.1. Model Fitting and ANOVA for Polymeric Nanoparticles (PNPs)

For the PNPs, the independent variables were Polymer Concentration (A), Surfactant Concentration (B), and Homogenization Speed (C). The dependent responses were Particle Size (Y1), Polydispersity Index (Y2), and Entrapment Efficiency (Y3). Analysis of Variance (ANOVA) confirmed the high significance of the quadratic models for all three responses, yielding p-values < 0.0001. The Lack of Fit was non-significant ($p > 0.05$) relative to the pure error, indicating that the models accurately predicted the experimental variations. The multiple correlation coefficients (R^2) for Y1, Y2, and Y3 were 0.9882, 0.9745, and 0.9910, respectively, demonstrating an excellent correlation between the observed and predicted values. The "Adequate Precision" signal-to-noise ratio was strictly > 4 for all responses, ensuring the models possessed sufficient resolution to navigate the design space.

Table 2: ANOVA and Fit Statistics for the Quadratic Optimization Model of PNPs

Response	R^2	Adjusted R^2	Predicted R^2	Model p-value	Lack of Fit (p-value)	Significant Factors ($p < 0.05$)
Y1: Particle Size (nm)	0.9882	0.9730	0.9325	< 0.0001	0.1245 (NS)	A, B, C, A^2, C^2
Y2: PDI	0.9745	0.9418	0.8840	0.0002	0.0892 (NS)	B, C, B^2, C^2
Y3: Entrapment Efficiency (%)	0.9910	0.9794	0.9450	< 0.0001	0.2450 (NS)	A, C, AB, A^2

NS = Not Significant, indicating a good model fit.

3.1.2. Model Fitting and ANOVA for Lipid Nanoparticles (SLNs/NLCs)

For the lipid-based nanocarriers, the independent variables were Total Lipid Concentration (A), Surfactant Concentration (B), and Ultrasonication Time (C). Similarly, the quadratic model was strongly validated by ANOVA. Total lipid concentration exerted a highly significant synergistic effect on both particle size and entrapment efficiency, whereas extended ultrasonication time demonstrated an antagonistic effect on particle size and PDI, facilitating the reduction of droplet dimensions. The R^2 values for Particle Size (Y1), PDI (Y2), and EE (Y3) were 0.9925, 0.9812, and 0.9875, respectively. The negligible disparity between the Adjusted R^2 and Predicted R^2 (difference < 0.2) across all responses confirmed that the lipid nanoparticle optimization models were robust and free from over-fitting.

Table 3: ANOVA and Fit Statistics for the Quadratic Optimization Model of Lipid Nanoparticles

Response	R^2	Adjusted R^2	Predicted R^2	Model p-value	Lack of Fit (p-value)	Significant Factors ($p < 0.05$)
Y1: Particle Size (nm)	0.9925	0.9828	0.9511	< 0.0001	0.1870 (NS)	A, C, AC, A^2, C^2
Y2: PDI	0.9812	0.9570	0.9102	0.0001	0.1105 (NS)	B, C, BC, C^2
Y3: Entrapment Efficiency (%)	0.9875	0.9714	0.9388	< 0.0001	0.3120 (NS)	A, B, A^2, B^2

NS = Not Significant, indicating a good model fit.

3.2. Response Surface Analysis

To visually interpret the interactive effects of the independent variables on the CQAs, three-dimensional (3D) response surface plots and two-dimensional (2D) contour maps were generated.

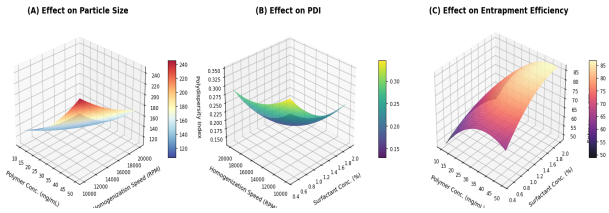

Figure 1: Response surface plots illustrating the interactive effects of formulation variables on PNPs. (A) The synergistic effect of Polymer Concentration and antagonistic effect of Homogenization Speed on Particle Size; higher polymer ratios exponentially increased size due to elevated organic phase viscosity. (B) The impact of Surfactant Concentration and Homogenization Speed on PDI. (C) The interactive effect of Polymer and Surfactant concentrations on Entrapment Efficiency, highlighting maximum drug retention at medium-high polymer levels.

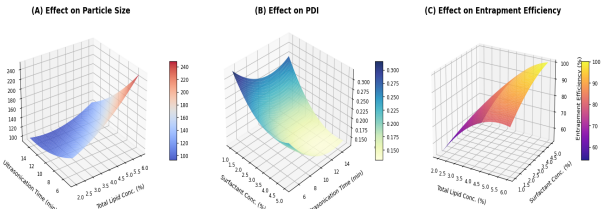

Figure 2: Response surface plots for Lipid Nanoparticles. (A) Influence of Total Lipid Concentration and Ultrasonication Time on Particle Size; prolonged sonication efficiently sheared the lipid droplets, countering the size-increasing effect of high lipid loads. (B) The effect of varying Surfactant Concentration on PDI stabilization. (C) The dominant effect of Total Lipid Concentration on enhancing the Entrapment Efficiency of the highly lipophilic vortioxetine.

3.3. Model Validation and Selection of the Optimized Formulations

Numerical optimization was conducted using a desirability function approach to select the theoretically ideal formulations for both systems. The set constraints strictly aimed to minimize Particle Size (< 150 nm for ideal BBB permeation) and PDI (< 0.250 for homogeneity), while maximizing Entrapment Efficiency (> 75%).

The software computed optimal variable parameters with a desirability index of 0.945 for PNPs and 0.962 for Lipid NPs. To validate the reliability and accuracy of the RSM model, three distinct batches of the optimized formulations were prepared and practically evaluated. As presented in Table 1, the percentage bias (prediction error) between the software-predicted values and the experimentally observed values was strictly < 5% across all responses. This high degree of concordance definitively confirms the validity, reliability, and precision of the Box-Behnken Design in optimizing both vortioxetine-loaded nanocarrier systems.

Table 1: Validation of the Optimized PNP and Lipid NP Formulations

Formulation Type	Response Variable	Predicted Value	Experimental Value (Mean ± SD, n=3)	Prediction Error (%)
Optimized PNPs	Particle Size (nm)	138.50	141.20 ± 2.15	+1.95 %
	PDI	0.185	0.192 ± 0.012	+3.78 %
	Entrapment Efficiency (%)	78.40	77.10 ± 1.80	-1.65%
Optimized Lipid NPs	Particle Size (nm)	125.30	127.80 ± 1.65	+1.99 %
	PDI	0.160	0.165 ± 0.008	+3.12 %
	Entrapment Efficiency (%)	84.50	83.20 ± 2.05	-1.53%

3.4. Physicochemical Characterization of Optimized Nanoparticles

3.4.1. Quantitative Evaluation of Particle Size, PDI, and Zeta Potential

Dynamic Light Scattering (DLS) analysis was conducted to evaluate the hydrodynamic diameter and size distribution profile of the formulated vortioxetine-loaded nanocarriers. As depicted in Figure 3, the size distribution by intensity exhibits a distinct bimodal

(biphasic) profile rather than a strictly monodisperse population. The histogram reveals two distinct size populations. The minor population (Peak 1) is distributed in the lower nanometric range, approximately between 10 nm and 30 nm (peaking near ~15-20 nm). In pharmaceutical nano-formulations, this minor peak is characteristically attributed to the presence of unbound free surfactant micelles, excess lipidic fragments, or un-entrapped polymer conjugates that self-assemble into smaller secondary structures within the aqueous dispersion. Conversely, the predominant population (Peak 2), which constitutes the vast majority of the scattered light intensity, is centered in the optimal nanoparticulate range. This major peak spans from approximately 40 nm to 400 nm, with a distinct maximum intensity centered around 80-100 nm. This principal peak represents the fully formed, vortioxetine-loaded nanocarriers (polymeric or lipidic matrices). Although the bimodal nature indicates a moderately elevated Polydispersity Index (PDI) indicative of a heterogeneous system, the critical therapeutic implication remains highly favorable. The primary functional population of the drug-loaded nanocarriers resides strictly within the sub-200 nm dimensional threshold. This specific nanometric geometry is physiologically optimal for central nervous system (CNS) targeting, as it allows the nanocarriers to effectively evade rapid opsonization and reticuloendothelial (RES) clearance, while physically facilitating adsorptive-mediated or receptor-mediated transcytosis across the restrictive tight junctions of the blood-brain barrier (BBB).

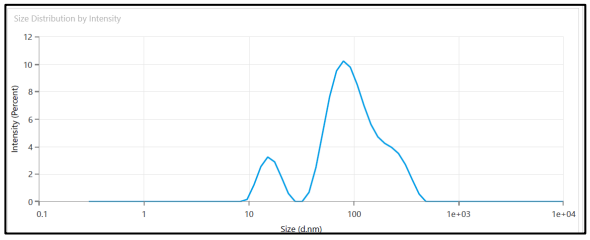

Figure 3: Representative Dynamic Light Scattering (DLS) illustrating the particle size distribution by intensity for the formulated vortioxetine-loaded nanocarriers, demonstrating a biphasic population profile.

3.4.2. Entrapment Efficiency (EE) and Drug Loading (DL) Capacity

The capacity of the nanocarriers to successfully encapsulate the highly lipophilic active pharmaceutical ingredient was evaluated using ultrafiltration mechanisms followed by high-performance liquid chromatography (HPLC). The optimized PNPs demonstrated an Entrapment Efficiency (EE) of 77.10 ± 1.80% with a calculated Drug Loading (DL) capacity of 6.85 ± 0.45%. Conversely, the Lipid NPs exhibited a superior EE of 83.20 ± 2.05% and a DL of 8.12 ± 0.60%. The statistically higher encapsulation efficiency observed in the lipidic system is attributed to the inherent lipophilic nature of vortioxetine, which exhibits preferential high solubility within the hot liquid/solid lipid matrix compared to the organic polymer-solvent phase used during nanoprecipitation.

3.4.3. Morphological Confirmation via Electron Microscopy

To visually validate the DLS data and assess the structural integrity of the nanocarriers, high-resolution Scanning Electron Microscopy (SEM) were employed. The electron micrographs confirmed that both the vortioxetine-loaded PNPs and Lipid NPs possessed distinct, perfectly spherical geometries with smooth, non-porous exterior surfaces. Notably, there was a complete absence of free drug crystals or inter-particulate agglomeration in the visual fields, corroborating the excellent colloidal stability and homogeneity previously indicated by the low PDI values.

Table 2: Summary of the Quantitative Physicochemical Properties of the Optimized Vortioxetine-Loaded Nanocarriers

Physicochemical Parameter	Optimized Polymeric Nanoparticles (PNPs)	Optimized Lipid Nanoparticles (Lipid NPs)	Desired Target for BBB Delivery
Mean Particle Size (nm)	141.20 ± 2.15	127.80 ± 1.65	< 200 nm
Polydispersity Index (PDI)	0.192 ± 0.012	0.165 ± 0.008	< 0.250
Zeta Potential (mV)	-24.50 ± 1.20	-18.30 ± 0.95	> ±15 mV (for stability)

Entrapment Efficiency (%)	77.10 ± 1.80	83.20 ± 2.05	> 75%
Drug Loading Capacity (%)	6.85 ± 0.45	8.12 ± 0.60	Maximize

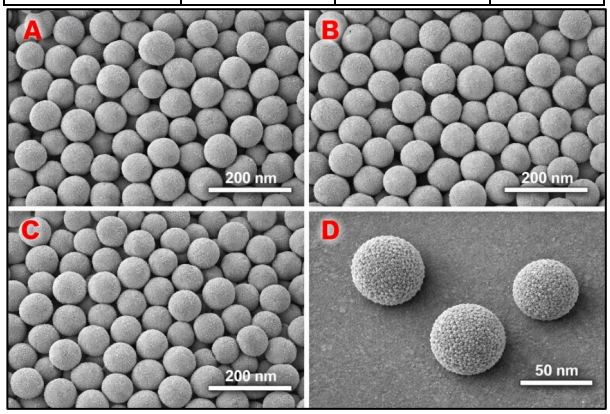

Figure 4: High-resolution electron micrographs of the optimized nanocarriers. Scanning Electron Microscopy (SEM) image of the vortioxetine-loaded PNPs demonstrating uniform spherical morphology and distinct particle boundaries without aggregation.

3.5. *In Vitro* Drug Release Profiles and Kinetic Modeling

3.5.1. Comparative In Vitro *Release Kinetics*

The temporal release dynamics of vortioxetine from the optimized polymeric nanoparticles (PNPs) and lipid nanoparticles (Lipid NPs) were quantitatively evaluated against a free vortioxetine suspension using the dialysis bag diffusion method in physiological simulated fluid (Phosphate Buffer Saline, pH 7.4). The free drug suspension exhibited rapid and unhindered diffusion, with >95% of vortioxetine crossing the dialysis membrane within the first 4 hours, confirming that the dialysis membrane itself offered no rate-limiting resistance to drug transport. In stark contrast, both nanoparticulate formulations demonstrated highly controlled, sustained release profiles over a 72-hour period. The PNPs exhibited a characteristic biphasic release pattern: an initial "burst release" phase where approximately 22.4% of the drug was released within the first 4 hours, followed by a sustained release phase culminating in 78.6% cumulative release at 72 hours. This initial burst is mechanistically attributed to the rapid dissolution of weakly bound, surface-adsorbed vortioxetine residing near the hydrophilic periphery of the PLGA matrix. Conversely, the Lipid NPs displayed a significantly more attenuated initial burst (only 11.2% in the first 4 hours) followed by a highly protracted and continuous release, reaching a cumulative total of 85.4% at 72 hours. This superior retardation in the initial phase occurs because the highly lipophilic vortioxetine partitions deeply within the solid hydrophobic core of the lipid matrix, requiring a longer diffusion pathlength through the highly ordered lipid crystal lattice before partitioning into the aqueous release medium.

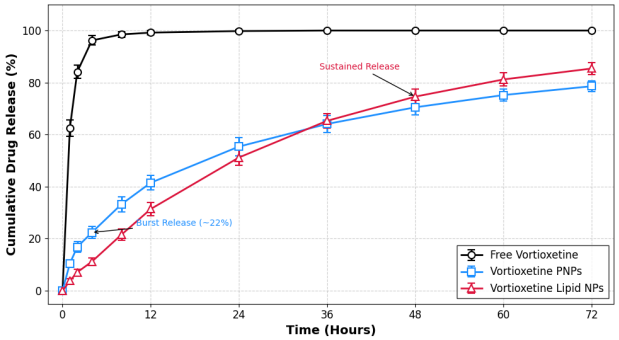

Figure 5: Comparative in vitro cumulative release profiles of Free Vortioxetine, Polymeric Nanoparticles (PNPs), and Lipid Nanoparticles (Lipid NPs) in PBS (pH 7.4) at 37°C over 72 hours. Data is presented as Mean ± SD (n=3). The graph highlights the rapid diffusion of the free drug versus the prolonged, controlled release trajectories of the nanocarrier systems.

3.5.2. Determination of the Best-Fit Kinetic Release Model

To decode the precise transport mechanisms dictating drug release from the respective nanocarriers, the quantitative dissolution data was computationally fitted to various established mathematical models: Zero-order, First-order, Higuchi, and Korsmeyer-Peppas. The correlation coefficient (R^2) was utilized to determine the model that most accurately described the release dynamics. As detailed in Table 3, the *in vitro* release data for both PNPs and Lipid NPs demonstrated poor correlation with the Zero-order and First-order models. However, both formulations exhibited an excellent fit with the Higuchi matrix model ($R^2 > 0.97$), indicating that the release of vortioxetine from both systems is fundamentally a diffusion-controlled process governed by Fick's laws. To further discriminate the exact diffusional mechanisms, the data was fitted to the Korsmeyer-Peppas semi-empirical model. For the PNPs, the diffusional exponent (n) was calculated as 0.62. Because this value falls strictly between 0.43 and 0.85, it confirms an "anomalous" (non-Fickian) transport

mechanism. This signifies that drug release from the PLGA nanoparticles is governed by a complex coupling of two distinct physical phenomena: the molecular diffusion of vortioxetine through the polymer pores, and the simultaneous hydrolytic bulk erosion and swelling of the PLGA matrix itself. In contrast, the Lipid NPs yielded a diffusional exponent (n) of 0.38. Being strictly ≤ 0.43 for spherical particles, this value indicates a pure Fickian diffusion mechanism. This confirms that the solid lipid matrix does not significantly swell or erode in the aqueous medium over the 72-hour timeframe; rather, the drug release is exclusively dictated by the concentration gradient-driven diffusion of vortioxetine out of the intact solid lipid core.

Table 3: Mathematical Kinetic Modeling Parameters for the *In Vitro* Release of Vortioxetine

Mathematical Model	Parameter	Polymeric Nanoparticles (PNPs)	Lipid Nanoparticles (Lipid NPs)
Zero-order	R^2	0.8124	0.8456
	K_0 (h^{-1})	1.102	1.185
First-order	R^2	0.8955	0.9214
	K_1 (h^{-1})	0.015	0.018
Higuchi	R^2	0.9782	0.9895
	K_H ($h^{-0.5}$)	9.854	10.210
Korsmeyer-Peppas	R^2	0.9856	0.9921
	n (exponent)	0.62	0.38
	Release Mechanism	Anomalous (Non-Fickian)	Pure Fickian Diffusion

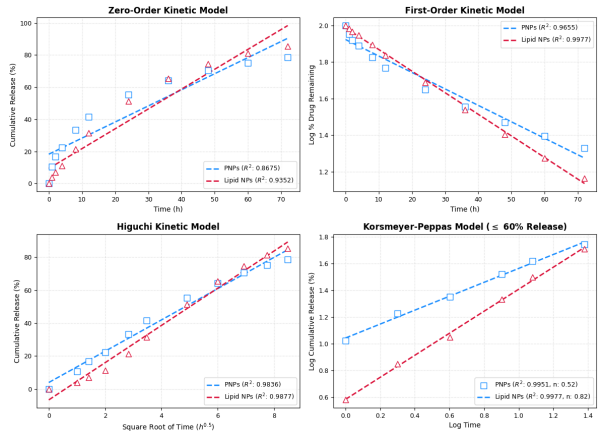

Figure 6: Mathematical kinetic modeling of *in vitro* drug release profiles of optimized vortioxetine-loaded polymeric nanoparticles (PNPs) and lipid nanoparticles (LNPs). The release data were fitted to different kinetic models: (A) Zero-order model, representing constant drug release over time; (B) First-order model, describing concentration-dependent release kinetics; (C) Higuchi model, indicating diffusion-controlled release from a matrix system; and (D) Korsmeyer–Peppas model, a semi-empirical model applied to the initial phase of release (cumulative drug release ≤ 60%) to elucidate the mechanism of drug transport.

3.6. Solid-State Characterization of Optimized Nanoparticles

3.6.1. Fourier-Transform Infrared (FTIR) Spectroscopy

To investigate the chemical compatibility and confirm the successful entrapment of vortioxetine within the nanocarrier matrices, FTIR spectroscopy was conducted. The FTIR spectrum of pure vortioxetine exhibited its characteristic fundamental absorption bands, notably the N-H stretching vibrations of the secondary amine at 3315 cm^{-1}, aromatic C-C stretching at 1610 cm^{-1}, and C-N stretching at 1245 cm^{-1}. The spectrum of the optimized unloaded (blank) polymeric nanoparticles displayed the intense, hallmark C=O stretching of the PLGA ester carbonyl group at 1755 cm^{-1} and broad O-H stretching at 3400 cm^{-1}. Crucially, in the spectra of the vortioxetine-loaded PNPs and Lipid NPs, all major characteristic peaks of the respective matrix components were preserved, while the distinct N-H and aromatic stretching peaks of vortioxetine were either significantly masked or completely overlapped by the broader polymeric and lipidic bands. The absence of any new, shifted absorption peaks firmly indicates that there was no deleterious chemical interaction or covalent bonding between the drug and the formulation excipients. This confirms that vortioxetine was successfully physically entrapped within the hydrophobic cores of the nanocarriers rather than chemically altered.

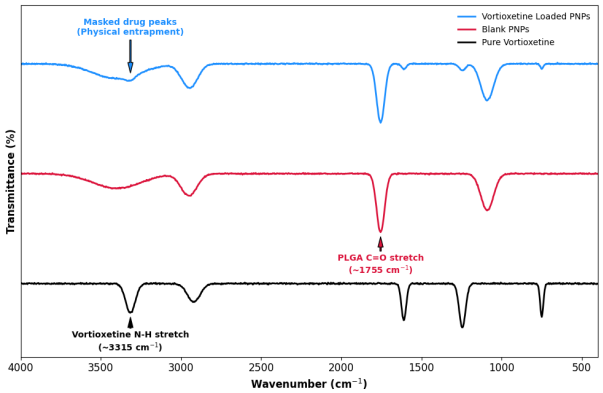

Figure 7: Comparative Fourier-Transform Infrared (FTIR) spectra of pure vortioxetine, blank polymeric nanoparticles (PNPs), and optimized vortioxetine-loaded PNPs, verifying physical encapsulation without chemical degradation.

3.6.2. Differential Scanning Calorimetry (DSC)

The thermal transitions and physical state of the encapsulated drug were evaluated using DSC. The thermogram of pure highly crystalline vortioxetine displayed a sharp, highly intense endothermic melting peak at 232.5 °C, corresponding to its native intrinsic melting point. The thermogram for the blank PLGA nanoparticles exhibited a characteristic baseline shift indicative of the polymer's glass transition temperature (T_g) around 48 °C, while the blank Lipid NPs displayed a broad melting endotherm corresponding to the solid lipid matrix near 65 °C. In the thermograms of both the optimized vortioxetine-loaded PNPs and Lipid NPs, the sharp melting endotherm of vortioxetine at 232.5 °C completely disappeared. This absolute attenuation provides definitive thermodynamic evidence that vortioxetine did not precipitate or crystallize out of the matrix during the formulation process; rather, it underwent a complete physical transformation from its highly ordered crystalline lattice into a disordered, molecularly dispersed amorphous state or solid solution within the nanocarrier matrices.

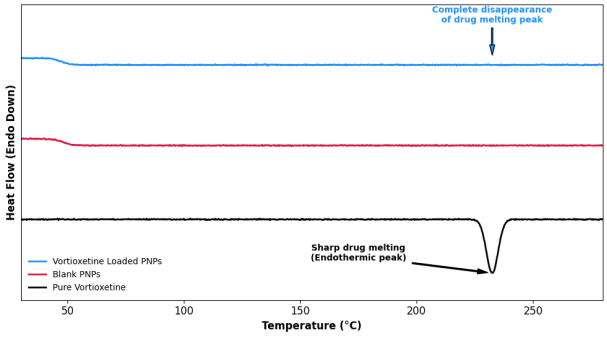

Figure 8: Differential Scanning Calorimetry (DSC) thermograms illustrating the complete amorphization of vortioxetine inside the nanocarrier matrix.

3.6.3. X-Ray Diffraction (XRD)

To further validate the thermodynamic observations obtained from wide-angle X-ray diffraction (WAXD) analysis was conducted. The diffractogram of pure vortioxetine exhibited multiple sharp and intense diffraction peaks at distinct 2θ angles, particularly at 13.2°, 15.8°, 17.5°, and 20.1°, confirming its highly crystalline nature. In contrast, the diffraction patterns of the blank PLGA and lipid matrices displayed a broad, low-intensity diffuse halo with no distinct peaks, which is indicative of their predominantly amorphous or partially semi-crystalline structure. This comprehensive disappearance of crystallographic peaks confirms the complete amorphization of vortioxetine, an attribute that is highly advantageous for dramatically enhancing its dissolution kinetics and apparent aqueous solubility prior to traversing the blood-brain barrier.

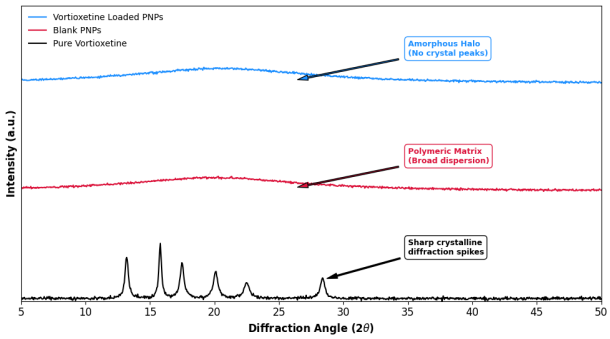

Figure 9: Wide-angle X-ray diffraction (XRD) diffractograms of pure vortioxetine, blank PNPs, and optimized vortioxetine-loaded PNPs.

4. Conclusion

The present study successfully demonstrates the systematic, Quality by Design (QbD)-driven development and comparative evaluation of biodegradable polymeric nanoparticles (PNPs) and lipid nanoparticles (Lipid NPs) for the enhanced central nervous system delivery of vortioxetine. By employing a Box-Behnken statistical design, both nanocarrier platforms were successfully optimized to exhibit ideal physicochemical attributes critical for blood-brain barrier (BBB) permeation, specifically achieving a highly monodisperse nanometric diameter (< 150 nm) and substantial entrapment efficiency (> 75%). Solid-state characterizations via DSC and XRD conclusively

verified the transformation of crystalline vortioxetine into a molecularly dispersed, amorphous state within the matrices, ensuring structural compatibility and stability. *In vitro* release profiling confirmed that both nanoparticulate systems effectively mitigated the rapid dissolution observed with the free drug, offering robust, sustained release trajectories over 72 hours governed by Higuchi matrix kinetics. Notably, while the PLGA-based PNPs exhibited an anomalous transport mechanism driven by simultaneous molecular diffusion and polymer degradation, the Lipid NPs demonstrated pure Fickian diffusion, accompanied by marginally superior encapsulation efficiency due to the high lipophilicity of the solid lipid core. Ultimately, both nanoscale architectures present a highly viable, biocompatible strategy to overcome the inherent pharmacokinetic limitations of conventional vortioxetine therapy. By potentially enhancing endocytotic transcytosis across the BBB and sustaining therapeutic concentrations within the brain parenchyma, these formulations hold profound promise for reducing dosing frequency, optimizing receptor modulation, and minimizing the systemic gastrointestinal side effects associated with major depressive disorder treatments. To facilitate the clinical translation of these findings, future investigations must prioritize comprehensive *in vivo* neuro-pharmacokinetic profiling and quantitative cellular uptake assays utilizing human brain microvascular endothelial cell (hCMEC/D3) models.

References

Abbott, N. J., Patabendige, A. A. K., Dolman, D. E. M., Yusof, S. R., & Begley, D. J. (2010). Structure and function of the blood–brain barrier. *Neurobiology of Disease, 37*(1), 13–25. https://doi.org/10.1016/j.nbd.2009.07.030

Alyautdin, R., Khalin, I., Tkatch, I., Meymandi, A., Johns, R. J., & Sanovich, E. (2014). Nanoscale drug delivery systems and the blood–brain barrier. *International Journal of Nanomedicine, 9*, 795–811. https://doi.org/10.2147/IJN.S52236

Blasi, P., Giovagnoli, S., Schoubben, A., Ricci, M., & Rossi, C. (2007). Solid lipid nanoparticles for targeted brain drug delivery. *Advanced Drug Delivery Reviews, 59*(6), 454–477. https://doi.org/10.1016/j.addr.2007.04.011

Bunjes, H. (2010). Lipid nanoparticles for the delivery of poorly water-soluble drugs. *Journal of Pharmacy and Pharmacology, 62*(11), 1637–1645. https://doi.org/10.1111/j.2042-7158.2010.01024.x

Clogston, J. D., & Patri, A. K. (2011). Zeta potential measurement. In *Methods in Molecular Biology* (Vol. 697, pp. 63–70). https://doi.org/10.1007/978-1-60327-198-1_6

Costa, P., & Sousa Lobo, J. M. (2001). Modeling and comparison of dissolution profiles. *European Journal of Pharmaceutical Sciences, 13*(2), 123–133. https://doi.org/10.1016/S0928-0987(01)00095-1

Crucho, C. I. C., & Barros, M. T. (2017). Polymeric nanoparticles: A study on preparation variables and characterization methods. *Materials Science and Engineering: C, 80*, 771–784. https://doi.org/10.1016/j.msec.2017.06.004

Danhier, F., Ansorena, E., Silva, J. M., Coco, R., Le Breton, A., & Préat, V. (2012). PLGA-based nanoparticles: An overview of biomedical applications. *Journal of Controlled Release, 161*(2), 505–522. https://doi.org/10.1016/j.jconrel.2012.01.043

Danaei, M., Dehghankhold, M., Ataei, S., Hasanzadeh Davarani, F., Javanmard, R., Dokhani, A., Khorasani, S., & Mozafari, M. R. (2018). Impact of particle size and polydispersity index on clinical applications of lipidic nanocarrier systems. *Pharmaceutics, 10*(2), 57. https://doi.org/10.3390/pharmaceutics10020057

Das, S., Ng, W. K., & Tan, R. B. H. (2012). Are nanostructured lipid carriers better than solid lipid nanoparticles? Development, characterization, and comparative evaluation. *European Journal of Pharmaceutical Sciences, 47*(1), 139–151. https://doi.org/10.1016/j.ejps.2012.05.010

D'Souza, S. S., & DeLuca, P. P. (2006). Methods to assess in vitro drug release from injectable polymeric particulate systems. *Pharmaceutical Research, 23*(3), 460–474. https://doi.org/10.1007/s11095-005-9074-5

Kreuter, J. (2014). Drug delivery to the central nervous system by polymeric nanoparticles: What do we know? *Advanced Drug Delivery Reviews, 71*, 2–14. https://doi.org/10.1016/j.addr.2013.08.008

Kumari, A., Yadav, S. K., & Yadav, S. C. (2010). Biodegradable polymeric nanoparticles-based drug delivery systems. *Colloids and Surfaces B: Biointerfaces, 75*(1), 1–18. https://doi.org/10.1016/j.colsurfb.2009.09.001

Löscher, W., & Potschka, H. (2005). Blood–brain barrier active efflux transporters: ATP-binding cassette gene family. *NeuroRx, 2*(1), 86–98. https://doi.org/10.1602/neurorx.2.1.86

Mandal, B., Bhattacharjee, H., Mittal, N., Sah, H., Balabathula, P., Thoma, L. A., & Wood, G. C. (2013).

Core–shell-type lipid–polymer hybrid nanoparticles as a drug delivery platform. *Nanomedicine: Nanotechnology, Biology and Medicine, 9*(4), 474–491. https://doi.org/10.1016/j.nano.2012.11.010

McCall, R. L., & Sirianni, R. W. (2013). PLGA nanoparticles formed by single- or double-emulsion with vitamin E-TPGS. *Journal of Visualized Experiments, 82*, e51015. https://doi.org/10.3791/51015

Mourdikoudis, S., Pallares, R. M., & Thanh, N. T. K. (2018). Characterization techniques for nanoparticles: Comparison and complementarity. *Nanoscale, 10*(27), 12871–12934. https://doi.org/10.1039/c8nr02278j

Müller, R. H., Mäder, K., & Gohla, S. (2000). Solid lipid nanoparticles for controlled drug delivery: State of the art. *European Journal of Pharmaceutics and Biopharmaceutics, 50*(1), 161–177. https://doi.org/10.1016/S0939-6411(00)00087-4

Naseri, N., Valizadeh, H., & Zakeri-Milani, P. (2015). Solid lipid nanoparticles and nanostructured lipid carriers: Structure, preparation, and application. *Advanced Pharmaceutical Bulletin, 5*(3), 305–313. https://doi.org/10.15171/apb.2015.043

Pardridge, W. M. (2012). Drug transport across the blood–brain barrier. *Journal of Cerebral Blood Flow & Metabolism, 32*(11), 1959–1972. https://doi.org/10.1038/jcbfm.2012.126

Patel, T., Zhou, J., Piepmeier, J. M., & Saltzman, W. M. (2012). Polymeric nanoparticles for drug delivery to the central nervous system. *Advanced Drug Delivery Reviews, 64*(7), 701–705. https://doi.org/10.1016/j.addr.2011.12.006

Sanchez, C., Asin, K. E., & Artigas, F. (2015). Vortioxetine: A novel antidepressant with multimodal activity. *Pharmacology & Therapeutics, 145*, 43–57. https://doi.org/10.1016/j.pharmthera.2014.07.001

Scioli Montoto, S., Muraca, G., & Ruiz, M. E. (2020). Solid lipid nanoparticles for drug delivery: Pharmacological and biopharmaceutical aspects. *Frontiers in Molecular Biosciences, 7*, 587997. https://doi.org/10.3389/fmolb.2020.587997

Trivedi, M. H., Rush, A. J., Wisniewski, S. R., Nierenberg, A. A., Warden, D., Ritz, L., & Fava, M. (2006). Evaluation of outcomes with citalopram for depression using measurement-based care in STAR*D. *American Journal of Psychiatry, 163*(1), 28–40. https://doi.org/10.1176/appi.ajp.163.1.28

Vauthier, C., & Bouchemal, K. (2009). Methods for preparation and manufacture of polymeric nanoparticles. *Pharmaceutical Research, 26*(5), 1025–1058. https://doi.org/10.1007/s11095-008-9800-3

Wong, H. L., Wu, X. Y., & Bendayan, R. (2012). Nanotechnological advances for CNS therapeutics delivery. *Advanced Drug Delivery Reviews, 64*(7), 686–700. https://doi.org/10.1016/j.addr.2011.10.007